The Astrophysical Journal Letters, 918:L5 (8pp), 2021 September 1 https://doi.org/10.3847/2041-8213/ac1922

Periodic Activities of Repeating Fast Radio Bursts from Be/X-Ray Binary Systems

Qiao-Chu Li[1,2], Yuan-Pei Yang[3], F. Y. Wang[1,2], Kun Xu[4,5], Yong Shao[1,2], Ze-Nan Liu[1,2], and Zi-Gao Dai[6,1]
[1] School of Astronomy and Space Science, Nanjing University, Nanjing 210023, People's Republic of China
[2] Key Laboratory of Modern Astronomy and Astrophysics (Nanjing University), Ministry of Education, Nanjing 210023, People's Republic of China
[3] South-Western Institute for Astronomy Research, Yunnan University, Kunming 650500, People's Republic of China; ypyang@ynu.edu.cn
[4] School of Astronomy and Space Sciences, University of Chinese Academy of Sciences, Beijing, People's Republic of China
[5] Key Laboratory of Optical Astronomy, National Astronomical Observatories, Chinese Academy of Sciences, Beijing, People's Republic of China
[6] Department of Astronomy, School of Physical Sciences, University of Science and Technology of China, Hefei 230026, People's Republic of China
daizg@ustc.edu.cn
Received 2021 June 16; revised 2021 July 22; accepted 2021 July 29; published 2021 August 25

Abstract

The frequency-dependent periodic active window of the fast radio burst FRB 180916.J0158+65 (FRB 180916B) was observed recently. In this letter, we propose that a Be/X-ray binary (BeXRB) system, which is composed of a neutron star (NS) and a Be star with a circumstellar disk, might be the source of a repeating FRB with periodic activities, and we apply this model to explain the activity window of FRB 180916B. The interaction between the NS magnetosphere and the accreted material results in evolution of the spin period and the centrifugal force of the NS, leading to the change of the stress in the NS crust. When the stress of the crust reaches the critical value, a starquake occurs and further produces FRBs. The interval between starquakes is estimated to be a few days, which is smaller than the active window of FRB 180916B. When the NS moves out of the disk of the Be star, the interval between starquakes becomes much longer than the orbital period, which corresponds to the nonactive phase. In this model, due to the absorption of the disk of the Be star, a frequency-dependent active window would appear for the FRBs, which is consistent with the observed properties of FRB 180916B. And the contribution of the dispersion measure from the disk of the Be star is small. In addition, the location of FRB 180916B in the host galaxy is consistent with a BeXRB system.

Unified Astronomy Thesaurus concepts: Radio transient sources (2008); Pulsars (1306); Be stars (142); High mass x-ray binary stars (733); Accretion (14)

1. Introduction

Fast radio bursts (FRBs) are a kind of millisecond-duration radio transients with extremely high brightness temperatures (for reviews, see Cordes & Chatterjee 2019; Petroff et al. 2019; Platts et al. 2019; Zhang 2020b; Xiao et al. 2021). So far, hundreds of FRBs have been detected (e.g., Lorimer et al. 2007; Thornton et al. 2013; Spitler et al. 2016; Chatterjee et al. 2017; Bannister et al. 2019; Prochaska et al. 2019; Ravi et al. 2019; Marcote et al. 2020), and a part of them show repeating behaviors (e.g., Spitler et al. 2014; CHIME/FRB Collaboration et al. 2019; Kumar et al. 2019; Luo et al. 2020). Recently, a Galactic FRB, FRB 200428 (Bochenek et al. 2020; CHIME/FRB Collaboration et al. 2020b), was discovered from the magnetar SGR J1935+2154, which is associated with an X-ray burst (Mereghetti et al. 2020; Li et al. 2021; Ridnaia et al. 2021; Tavani et al. 2021). This indicates that magnetars are at least one origin of FRBs, while the radiation mechanism of FRBs might still be unclear (e.g., Lyubarsky 2014; Geng & Huang 2015; Dai et al. 2016; Kumar et al. 2017; Lyutikov 2017; Waxman 2017; Zhang 2017; Katz 2018; Yang & Zhang 2018, 2021; Metzger et al. 2019; Wadiasingh & Timokhin 2019; Beloborodov 2020; Dai 2020; Geng et al. 2020; Kumar & Bošnjak 2020; Lu et al. 2020; Wu et al. 2020; Xiao & Dai 2020; Yang et al. 2020; Zhang 2020b; Yu et al. 2021).

Remarkably, there are two repeating sources showing periodic activities: FRB 180916.J0158+65 (FRB 180916B), with a 16.35 day periodic activity and a 5 day activity window (CHIME/FRB Collaboration et al. 2020a), and FRB 121102, with a possible longer period of ∼160 days (Rajwade et al. 2020; Cruces et al. 2021) and an active window of about ∼100 days. Also, the possible periodic activities of the soft gamma-ray repeaters SGR 1806–20 and SGR J1935+2154 were found to be about 398.2 (Zhang et al. 2021) and 237 (Zou et al. 2021) days, respectively. Several scenarios have been proposed to explain the periodic activities of FRBs (see Zhang 2020a). First, the FRB source is in a binary system with the observed period corresponding to the orbital period of this binary system (Dai et al. 2016; Smallwood et al. 2019; Dai & Zhong 2020; Gu et al. 2020; Ioka & Zhang 2020; Lyutikov et al. 2020; Mottez et al. 2020; Decoene et al. 2021; Deng et al. 2021; Kuerban et al. 2021; Wada et al. 2021); second, the FRB is generated by the neutron star (NS) magnetosphere, and the observed periodic activities are due to the precession of the emitting region (Levin et al. 2020; Yang & Zou 2020; Zanazzi & Lai 2020; Tong et al. 2020; Li & Zanazzi 2021; Sridhar et al. 2021); third, the observed period is due to the rotation of a very slow NS (Beniamini et al. 2020; Xu et al. 2021); and fourth, the periodic activities originate from the thermal-viscous instability of the accretion disk around the compact star in a binary system, which produces the low/high accretion state corresponding to the quiescence/active phases (Geng et al. 2021).

Recently, FRB 180916B was found to be ∼250 pc offset from the brightest region of the nearest young stellar clump in its host galaxy, which is suggested to be the birthplace of FRB 180916B (Tendulkar et al. 2021). It would take 800 kyr to 7 Myr for FRB 180916B to cross the observed distance from this presumed birthplace, which is in tension with scenarios that invoke young ($\lesssim$10 kyr) magnetars formed in core-collapse supernovae (Tendulkar et al. 2021). However, such a large offset might be well consistent with the case of the high-mass X-ray binaries (HMXBs; Bodaghee et al. 2012). In particular, Pleunis et al. (2021) recently found that FRB 180916B is likely to be from an interacting binary featuring an NS and high-mass companion, which accounts for

most observational properties of this FRB. Therefore, the relation between FRBs and HMXBs should be extensively investigated.

Notably, there is a subtype of HMXB called the Be/X-ray binary (BeXRB), whose typical orbital period (∼10 days to 1 yr; Okazaki et al. 2002) is similar to the period of FRB 180916B. Meanwhile, the NS with a strong magnetic field ($\sim 10^{12}$–10^{13} G; Tauris & van den Heuvel 2006) in the BeXRB system could also be the central engine of FRBs. Recently, Zhang & Gao (2020) used the population synthesis method to study in detail the properties of the companion star, aiming to explain the periodicity of FRB 180916B. They found that the companion star is most likely to be a B-type star. The classical Be star is a main-sequence B star, which rotates so fast that an outwardly diffusing gaseous, dust-free Keplerian disk is formed (Okazaki & Negueruela 2001). The BeXRBs can exhibit X-ray radiation outbursts that last from a week to several months. One type of outburst is called normal outbursts or type I outbursts, which are characterized by an X-ray luminosity of $L_{\rm X} \sim 10^{36}$–10^{37} erg s^{-1}, periodically peaking at or close to the periastron, and covering 0.2–0.3 $P_{\rm orb}$ of the orbital period (e.g., Reig 2011). The origin of type I outbursts is usually explained by the accretion of the NS from the Be star disk, when the NS is approaching the Be star near the periastron (e.g., Okazaki & Negueruela 2001).

Up to now, with detections of FRB 180916B from 110 to 1765 MHz (Aggarwal et al. 2020; CHIME/FRB Collaboration et al. 2020a; Marthi et al. 2020; Pastor-Marazuela et al. 2020; Sand et al. 2020), the period is confirmed to be $16.29^{+0.15}_{-0.17}$ days, and the active window is 6.1 days, which peaks earlier at higher frequencies (Pastor-Marazuela et al. 2020). In this letter, we propose that a BeXRB system could be the source of a repeating FRB with periodic activity. We discuss the triggering mechanism of FRBs in a BeXRB and predict the waiting time and energy in Section 2.1. We use the BeXRB model to explain the frequency-dependent active window of FRB 180916B in Section 2.2. We calculate the dispersion measure (DM) contribution from the disk of the Be star and make a comparison with the observations of FRB 180916B in Section 2.3. Finally, we provide some discussion and conclusions in Section 3.

2. Repeating FRBs from a BeXRB System

In a BeXRB system (Figure 1(a)), the NS will accrete material when it is in the disk of the Be star (e.g., Okazaki & Negueruela 2001; Wilson-Hodge et al. 2018). The interaction between accreted material and the NS magnetosphere will change the spin period of the NS. In this scenario, FRBs might be triggered by starquakes due to the spin evolution of the NS. Different from the model that FRBs are triggered by magnetic stress evolution in the magnetar crust (Yang & Zhang 2021), for an NS with a relatively weaker magnetic field and faster spin, the crust fracturing would be adjusted by the balance between crust stress and centrifugal force. Because an NS may spin up or down during the interaction between its magnetosphere and the accreted material around the NS, the balance of the crust would be destroyed. The stress of the crust reaching a critical value will cause the crust to fracture. When the NS moves outside the Be disk, it will spin down by magnetic dipole or gravitational-wave radiation. In the following discussion, we will estimate the rates and energies of the starquakes when the NS is in/out of the Be star disk and study whether accretion-induced starquakes can provide enough energy and explain the high rate of repeating FRBs.

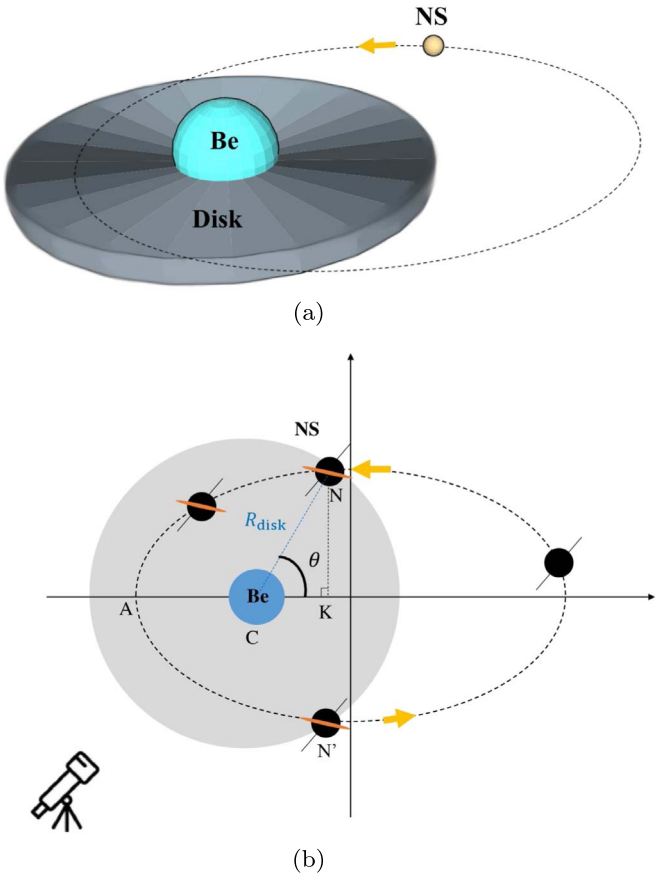

Figure 1. Schematic illustration of the BeXRB model in this work: (a) three-dimensional structure of the system with a Keplerian disk of the Be star, and the NS is coplanar with the disk; (b) top view of the system. The dotted ellipse represents the orbit of the NS. The gray area represents the disk of the Be star. In the disk accretion process, an accretion disk (the orange area) would form around the NS when it is in the circumstellar disk of the Be star and begin to fade during it is out of the circumstellar disk of the Be star (e.g., Okazaki & Negueruela 2001).

2.1. Repeating FRBs Triggered by NS Starquakes in a BeXRB System

First, we provide a discussion about starquakes of the NS induced by the spin evolution. When the spin period of the NS changes, the oblateness (ε) and moment of inertia (I) will change to readjust the stellar shape. The oblateness of the NS is defined as $\varepsilon \equiv |I - I_0|/I$, where the nonrotating moment of inertia of the NS is taken as $I_0 = 10^{45}$ g cm^2. The rigidity of the NS resists this change, and this corresponding energy is defined as the strain energy $E_{\rm strain} = \mathcal{B}(\varepsilon - \varepsilon_0)^2$, where $\mathcal{B}$ is the coefficient and ε_0 is a reference oblateness without strain energy. The mean stress is

$$\sigma = \left| \frac{1}{V} \frac{\partial E_{\rm strain}}{\partial \varepsilon} \right| = \mu |\varepsilon - \varepsilon_0|, \quad (1)$$

where V is the volume of the NS, and $\mu = 2\mathcal{B}/V$ is the mean shear modulus[7] of the NS. There is a critical stress value $\sigma_{\rm c}$, above which, i.e., $\sigma > \sigma_{\rm c}$, a starquake can take place.

[7] The shear modulus of the crust of the NS can be represented by (e.g., Thompson & Duncan 1995; Douchin & Haensel 2001; Piro 2005) $\mu \simeq 6.0 \times 10^{30}$ erg cm^{-3} $\rho_{\rm n}^{4/3}(Z/50)^2(615/A)^{4/3}[(1 - X_{\rm n})/0.4]^{4/3}$, where $\rho_{\rm n} = 2.8 \times 10^{14}$ g cm^{-3} is the nuclear density, Z is the number of protons per ion, A is the number of nucleons in a nucleus, and $X_{\rm n}$ denotes the fraction of neutrons outside the nuclei. Because the shear modulus of the NS crust during the accretion process is a little bit softer (e.g., Haensel & Zdunik 2008; Zdunik et al. 2008), here we adopt $\mu \sim 10^{31}$ erg cm^{-3} in this process.

The total energy of the NS can be estimated by (Baym & Pines 1971; Shapiro & Teukolsky 1983),

$$E = E_{\rm grav} + E_{\rm rot} + E_{\rm strain} = E_0 + \mathcal{A}\varepsilon^2 + \mathcal{L}^2/(2I) + \mathcal{B}(\varepsilon - \varepsilon_0)^2, \quad (2)$$

where $E_{\rm grav} = E_0 + \mathcal{A}\varepsilon^2$ is the gravitational energy of the rotating NS, with the energy of the nonrotating star $E_0 = -3M_{\rm NS}^2 G/(5R_{\rm NS})$ and the coefficient $\mathcal{A} = -1/5E_0$ for a self-gravitating incompressible sphere, and $E_{\rm rot} = \mathcal{L}^2/(2I)$ is the rotation energy, with the stellar angular momentum $\mathcal{L} = I\Omega$ and the angular velocity of the NS $\Omega = 2\pi/P_{\rm NS}$. By minimizing the total energy E, ε satisfies

$$\varepsilon = \frac{\Omega^2}{4(\mathcal{A}+\mathcal{B})}\frac{\partial I}{\partial \varepsilon} + \frac{\mathcal{B}}{\mathcal{A}+\mathcal{B}}\varepsilon_0 = \frac{I_0\Omega^2}{4(\mathcal{A}+\mathcal{B})} + \frac{\mathcal{B}}{\mathcal{A}+\mathcal{B}}\varepsilon_0, \quad (3)$$

where $\partial I(\varepsilon)/\partial\varepsilon = I_0$. By setting $\mathcal{B} = 0$, the reference oblateness is $\varepsilon_0 = I_0\Omega_0^2/(4\mathcal{A})$, where Ω_0 is the angular velocity of the NS with a completely unstressed crust.

When the stress σ in Equation (1) reaches the critical stress $\sigma_{\rm c}$, a starquake is produced. The reference oblateness as a reference point shifts $\Delta\varepsilon_0$, and thus the actual oblateness of the NS shifts

$$\Delta\varepsilon = \frac{\mathcal{B}}{\mathcal{A}+\mathcal{B}}\Delta\varepsilon_0. \quad (4)$$

According to the conservation of the angular momentum, $\Delta\varepsilon = |\Delta\Omega/\Omega|$, where $\Delta\Omega$ is the difference between the angular velocity after and before the starquake. Based on the observation of pulsar glitches, $\Delta\varepsilon$ can span several orders of magnitude, from $\Delta\varepsilon \approx 10^{-12}$ to 10^{-5} (Espinoza et al. 2011). Lai et al. (2018) gave an estimation of $\Delta\varepsilon \sim 10^{-10}$ for the Crab pulsar and $\Delta\varepsilon \sim 10^{-11}$ for the Vela pulsar from the observations (Espinoza et al. 2011). Then, the stress relieved during a starquake can be represented by

$$|\Delta\sigma| = \mu|\Delta\varepsilon_0 - \Delta\varepsilon| = \mu\frac{\mathcal{A}}{\mathcal{B}}|\Delta\varepsilon|. \quad (5)$$

According to Equations (1) and (3), the stress in the crust will start to build up again after the starquakes at a rate

$$|\dot\sigma| = \mu|\dot\varepsilon| = \frac{\mu I_0}{2(\mathcal{A}+\mathcal{B})}\Omega|\dot\Omega|, \quad (6)$$

where $\dot\Omega$ is the change rate of angular velocity of the NS. The next starquake occurs after a time (Haskell & Melatos 2015)

$$t_{\rm s} \approx \frac{|\Delta\sigma|}{|\dot\sigma|} = \frac{2\mathcal{A}(\mathcal{A}+\mathcal{B})|\Delta\varepsilon|}{\mathcal{B}I_0\Omega|\dot\Omega|}, \quad (7)$$

i.e., the waiting time of the NS starquakes, where $\dot\Omega$ can be derived by the torque N on the NS, i.e., $N = I_0\dot\Omega$. In the following, we will derive N on the NS in/out of the Be star disk.

Because the accretion process of the NS in a BeXRB system is still unclear, both disk accretion (e.g., Okazaki & Negueruela 2001; Xu & Li 2019) and wind accretion (e.g., Ikhsanov 2007; Shakura et al. 2012) are possible scenarios. When the NS is in the disk of the Be star, if the interaction radius between the accreted material and the NS magnetosphere $R_{\rm in}$ and the radius of the light cylinder $R_{\rm lc}$ satisfies $R_{\rm in} < R_{\rm lc} = c/\Omega \simeq 4.8\times10^7(P_{\rm NS}/0.01\ {\rm s})$ cm, there will exist an interaction between the accreted material and the magnetosphere of the NS. In this situation, an accretion torque $N_{\rm acc}$ would change the NS spin evolution, leading to spin-up or spin-down.[8] The $N_{\rm acc}$ can be represented by (e.g., Ghosh & Lamb 1979b; Lü et al. 2012)

$$N_{\rm acc} \simeq \pm\dot M(GM_{\rm NS}R_{\rm in})^{1/2}, \quad (8)$$

where $\dot M$ is the accretion rate of the NS, the plus sign corresponds to the spin-up case, and the minus sign corresponds to the spin-down case. The total torque can be represented by $N_{\rm tot} = N_{\rm acc} + N_{\rm rad}$, with the radiation torque of the NS being $N_{\rm rad}$. Because $|N_{\rm tot}| \gg |N_{\rm rad}|$, the starquakes in both the accretor and propeller states would have the same waiting time.[9]

The interaction radius between the accreted material and the NS magnetosphere $R_{\rm in}$ can be evaluated by $R_{\rm in} = \xi R_{\rm A}$. Here $\xi \sim 0.01$–1 is taken for the disk accretion (e.g., Ghosh & Lamb 1979a; Filippova et al. 2017), and $\xi \sim 1$ is taken for the wind accretion (e.g., Lü et al. 2012). The Alfvén radius $R_{\rm A} = [\mu_{\rm NS}^4/(2GM_{\rm NS}\dot M^2)]^{1/7}$ is where the magnetic pressure of an NS is equal to the shock pressure of accreted material, with the accretion rate $\dot M$. Here $\mu_{\rm NS} = B_{\rm NS}R_{\rm NS}^3/2$ is the magnetic moment of the NS, with the surface magnetic field of the NS being $B_{\rm NS}$. Thus, $R_{\rm in}$ is represented by

$$R_{\rm in} \simeq 4.1\times10^7\ {\rm cm}\left(\frac{\xi}{0.1}\right)\left(\frac{B_{\rm NS}}{10^{13}\ {\rm G}}\right)^{4/7}\left(\frac{R_{\rm NS}}{10^6\ {\rm cm}}\right)^{12/7} \times\left(\frac{\dot M}{\dot M_{\rm Edd}}\right)^{-2/7}\left(\frac{M_{\rm NS}}{1.4M_\odot}\right)^{-1/7}. \quad (9)$$

The Eddington luminosity is defined as $L_{\rm Edd} \equiv 4\pi GM_{\rm NS}m_{\rm p}c/\sigma_{\rm T}$, where $m_{\rm p}$ is the mass of the proton and $\sigma_{\rm T}$ is the Thompson cross section. The rate of Eddington accretion is $\dot M_{\rm Edd} \simeq 10^{18}(R_{\rm NS}/10^6\ {\rm cm})\ {\rm g\ s^{-1}}$. For BeXRB systems, the X-ray luminosity of the type I outbursts is about 10^{36}–$10^{37}\ {\rm erg\ s^{-1}}$. If we assume that all of the kinetic energy of the accretion matter is converted to the luminosity of type I outbursts, i.e., $L = 1/2\dot M v_{\rm ff}^2 = GM_{\rm NS}\dot M/R_{\rm NS}$, with a freefall velocity $v_{\rm ff} = \sqrt{2GM_{\rm NS}/R_{\rm NS}}$, we can derive that the accretion rate of the NS is about $0.1\dot M_{\rm Edd}$.

According to Equation (7), the waiting time of two starquakes induced by accretion of the NS in the Be star disk

[8] We define the corotation radius as $R_{\rm co}$, where the local Keplerian angular velocity of the accreted material equals the angular velocity of the NS. If $R_{\rm in} < R_{\rm co}$, i.e., the accretor state, the material in the inner boundary would be faster than the rotation velocity of the NS and flow along the magnetic field lines onto the NS (Frank et al. 2002), which causes accretion to occur and accelerates the rotation of the NS by the angular momentum transfer. If $R_{\rm co} < R_{\rm in} < R_{\rm lc}$, i.e., the propeller state, accretion is forbidden, because the velocity of the accretion disk is less than the rotation velocity of the NS. The material of the accretion disk is thrown out by centrifugal force, which takes away angular momentum and decelerates the NS.

[9] Here we only consider that the direction of the accretion disk of the NS is the same as that of the NS spin.

can be represented by

$$t_{\rm s} \simeq 2.5\ {\rm days}\left(\frac{\Delta\varepsilon}{10^{-13}}\right)\left(\frac{P_{\rm NS}}{0.01\ {\rm s}}\right)\left(\frac{\xi}{0.1}\right)^{-1/2} \times \left(\frac{B_{\rm NS}}{10^{13}\ {\rm G}}\right)^{-2/7}\left(\frac{\dot{M}}{\dot{M}_{\rm Edd}}\right)^{-6/7}, \quad (10)$$

with $\mu = 10^{31}\ {\rm erg\ cm^{-3}}$ (e.g., Thompson & Duncan 1995; Douchin & Haensel 2001; Piro 2005), $M_{\rm NS} = 1.4\ M_\odot$, $R_{\rm NS} = 1.2 \times 10^6$ cm, and $|N_{\rm acc}| \gg |N_{\rm dip}|$. Here we take $P_{\rm NS} = 0.01$ s as a reference value, which is consistent with the observation of SAX J0635+0533 with a spin period of 0.0338 s (Kaaret et al. 1999; Cusumano et al. 2000). If $P_{\rm NS} = 0.02$ s, $\Delta\varepsilon = 10^{-13}$, $\xi = 0.1$, $B_{\rm NS} = 10^{13}$ G, $M_{\rm NS} = 1.4\ M_\odot$, $R_{\rm NS} = 1.2 \times 10^6$ cm, and $\dot{M} = \dot{M}_{\rm Edd}$, we obtain $R_{\rm in} \simeq 5.3 \times 10^7$ cm $< R_{\rm lc} \simeq 9.5 \times 10^7$ cm and $t_{\rm s} \simeq 4.9$ days. Thus, in an active window of FRB 180916B, there would be several starquakes, leading to several FRBs occurring in the active window. If $\xi = 0.5$, $P_{\rm NS} = 0.01$ s, $B_{\rm NS} = 10^{13}$ G, $M_{\rm NS} = 1.4\ M_\odot$, $R_{\rm NS} = 1.2 \times 10^6$ cm, and $\dot{M} = \dot{M}_{\rm Edd}$, $R_{\rm in} \simeq 2.6 \times 10^8$ cm $> R_{\rm lc} \simeq 4.8 \times 10^7$ cm; without interaction between the accreted material and the magnetosphere of the NS, the NS will spin down through radiation, which will be discussed later.

When the crust of the NS cracks, the magnetic field near the surface will be disturbed and further propagate as Alfvén waves into the magnetosphere (e.g., Thompson & Duncan 1995; Kumar & Bošnjak 2020; Lu et al. 2020; Yang & Zhang 2021). The released energy can be evaluated by

$$E_{\rm s} \sim \zeta\frac{B_{\rm NS}^2}{8\pi}4\pi R_{\rm NS}^2\Delta R \simeq 5.0 \times 10^{42}\ {\rm erg}\ \zeta\left(\frac{B_{\rm NS}}{10^{13}\ {\rm G}}\right)^2 \times \left(\frac{R_{\rm NS}}{10^6\ {\rm cm}}\right)^2\left(\frac{\Delta R}{10^5\ {\rm cm}}\right), \quad (11)$$

where ΔR is the thickness of the crust and ζ is the magnetic energy conversion factor. Therefore, the energy released by the magnetic energy in the NS crust is enough to produce FRBs.

When the NS is outside the disk of the Be star or $R_{\rm in} > R_{\rm lc}$, the accretion will be very weak. Taking $|\dot{\Omega}| = 2\pi P_{\rm NS}^{-2}\dot{P}_{\rm NS}$ into Equation (7), the interval between two starquakes due to the radiation of the NS can be estimated by

$$t_{\rm s}^{'} \simeq 2774\ {\rm days}\left(\frac{\Delta\varepsilon}{10^{-13}}\right)\left(\frac{P_{\rm NS}}{0.01{\rm s}}\right)^3\left(\frac{\dot{P}_{\rm NS}}{10^{-18}{\rm ss}^{-1}}\right)^{-1}, \quad (12)$$

where $\dot{P}_{\rm NS}$ is the period derivative of the NS, with a typical value in the range 10^{-20} to 10^{-10} s s^{-1} (Taylor et al. 1993). The other parameters are taken as $\mu = 10^{31}\ {\rm erg\ cm^{-3}}$, $M_{\rm NS} = 1.4\ M_\odot$, and $R_{\rm NS} = 1.2 \times 10^6$ cm. This interval is much longer than the orbit period of the BeXRB system; thus, it is unlikely to produce radio bursts when the NS moves outside the disk of the Be star.

In Figure 2, we plot the parameter space of the period and magnetic field of the NS. The area enclosed by the red dashed line, purple dashed–dotted line, and blue dotted line satisfies $t_{\rm s} < 6.1$ days, $t_{\rm s}^{'} > 16.29$ days, and $R_{\rm in} < R_{\rm lc}$, which is suitable to explain FRB 180916B period activity. In this area, different colors denote different $t_{\rm s}$. The parameters are taken as $\mu = 10^{31}\ {\rm erg\ cm^{-3}}$, $\xi = 0.1$, $\Delta\varepsilon = 10^{-13}$, $\dot{M} = \dot{M}_{\rm Edd}$, $\dot{P}_{\rm NS} = 10^{-18}$ s s^{-1}, $M_{\rm NS} = 1.4\ M_\odot$, and $R_{\rm NS} = 1.2 \times 10^6$ cm.

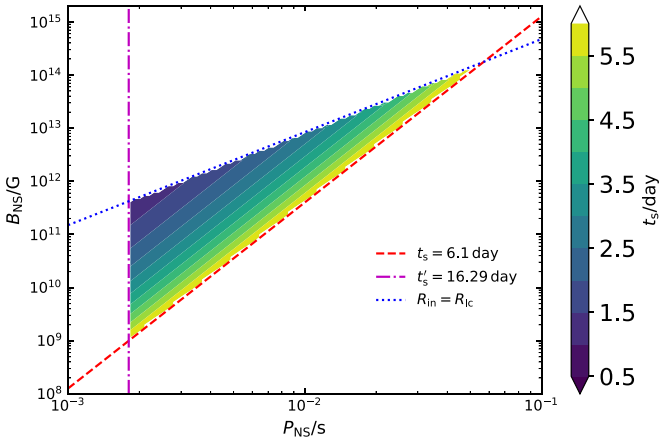

Figure 2. Period and magnetic field of the NS in a BeXRB system. The red dashed line, purple dashed–dotted line, and blue dotted line denote $t_{\rm s} = 6.1$ days, $t_{\rm s}^{'} = 16.29$ days, and $R_{\rm in} = R_{\rm lc}$, respectively. Thus, the enclosed area is the range that meets $t_{\rm s} < 6.1$ days, $t_{\rm s}^{'} > 16.29$ days, and $R_{\rm in} < R_{\rm lc}$. The darker the color, the shorter the $t_{\rm s}$. Model parameters are taken as $\xi = 0.1$, the shear modulus of the crust $\mu = 10^{31}\ {\rm erg\ cm^{-3}}$, the oblateness of the NS $\Delta\varepsilon = 10^{-13}$, the accretion rate $\dot{M} = \dot{M}_{\rm Edd}$, the period derivative of the NS $\dot{P}_{\rm NS} = 10^{-18}$ s s^{-1}, the mass of the NS $M_{\rm NS} = 1.4\ M_\odot$, and the radius of the NS $R_{\rm NS} = 1.2 \times 10^6$ cm.

When the crust fractures, Alfvén waves will be generated at the surface of the NS by the starquake and propagate into the magnetosphere, further producing FRBs at a large radius (Kumar & Bošnjak 2020; Lu et al. 2020; Yang & Zhang 2021). About tens of NS radius, the plasma density in the magnetosphere is not enough to screen the parallel electric field associated with the Alfvén wave, leading to a charge-starved region. In this scenario, FRBs could be emitted by bunching coherent curvature radiation due to two-stream instability (Kumar & Bošnjak 2020; Lu et al. 2020; Yang et al. 2020) or coherent plasma radiation (Yang & Zhang 2021).

2.2. Periodicity and Active Window of FRB 180916B

We assume that the disk of the Be star is coplanar with the orbit of the NS for simplicity, and FRBs are produced when the NS passes through the disk of the Be star. In Figure 1(b), the Be star is at the left focus of the orbit. The NS moves counterclockwise. Point N is where the NS starts to move into the disk of the Be star, and point N' is where the NS is beginning to move outside of the disk of the Be star. We define

$$\Delta S_{\rm NS}(\theta_1, \theta_2) \equiv \frac{1}{2}\int_{\theta_1}^{\theta_2}\left[\frac{a(1-e^2)}{1 - e\cos\theta}\right]^2 d\theta, \quad (13)$$

where θ is the azimuth angle of the NS relative to the Be star, a is the length of the semimajor axis of the orbit, and e is the orbital eccentricity. The area swept out by a line joining the Be star and the NS from point N to point N' can be calculated by $\Delta S_{\rm NS}(\theta_0,\ 2\pi - \theta_0)$, where θ_0 is the initial azimuth angle at point N. Setting the phase of the orbit periastron as 0.5, the phase at any azimuth angle, θ_x, of the orbit can be represented by $\phi(\theta_x) = \Delta S_{\rm NS}(\theta_0, \theta_x)/S_{\rm NS} - \Delta S_{\rm NS}(\theta_0, \pi)/S_{\rm NS} + 0.5$.

According to Kepler's third law, the length of the semimajor axis of the orbit should meet $a = [G(M_\star + M_{\rm NS})P_{\rm orb}^2/4\pi^2]^{1/3} \simeq 4.8 \times 10^{12}$ cm, where the orbit period is $P_{\rm orb} = 16.29$ days, the mass of the Be star is taken as $M_\star = 15\ M_\odot$, and the mass of the NS is $M_{\rm NS} = 1.4\ M_\odot$. The total area of the orbit is

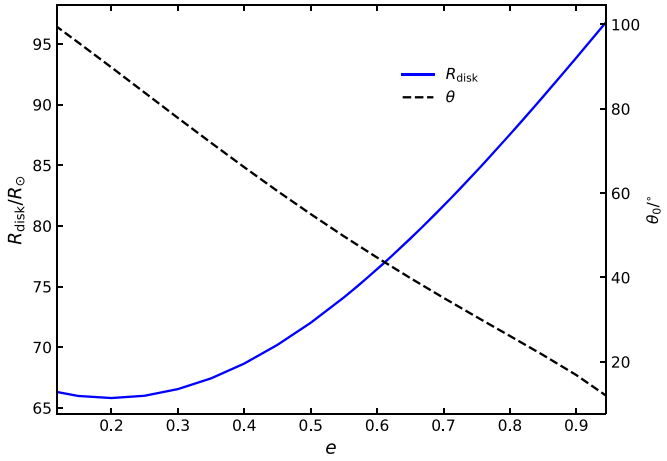

Figure 3. Radius of the disk of the Be star $R_{\rm disk}$ and the initial azimuth angle of the NS just entering the disk θ_0 as functions of the orbital eccentricity of the BeXRB e. The parameters are taken as $P_{\rm orb} = 16.29$ days and $\Delta P_{\rm orb} = 6.1$ days.

$S_{\rm NS} = \pi(1 - e^2)^{1/2}a^2$. We define the active fraction of the period as the duty cycle. According to Kepler's second law, the duty cycle can be represented by

$$\mathcal{D} \equiv \frac{\Delta P_{\rm orb}}{P_{\rm orb}} = \frac{\Delta S_{\rm NS}(\theta_0, 2\pi - \theta_0)}{S_{\rm NS}} = \frac{6.1 \text{ days}}{16.29 \text{ days}} \simeq 0.37, \tag{14}$$

with the active window of FRB 180916B being $\Delta P_{\rm orb}$.

The abscissa of point N satisfies $x_{\rm K} = (-a^2 + aR_{\rm disk})/c_{\rm e}$ and $x_{\rm K} = R_{\rm disk}\cos(\theta_0) - c_{\rm e}$, with $c_{\rm e}$ the focal length of the orbit and $R_{\rm disk}$ the radius of the disk. For a given orbit period and active window, $R_{\rm disk}$ and θ_0 are functions of e, respectively, as shown in Figure 3. When the eccentricity e is larger, a larger disk radius $R_{\rm disk}$ and smaller initial azimuth angle θ_0 are required.

Next, we establish a three-dimensional model to describe the density distribution of the Be star disk. The disk of the Be star is usually a Keplerian disk (e.g., Lee et al. 1991; Okazaki 1991; Quirrenbach et al. 1997; Rivinius et al. 2013). The velocity at the horizontal distance r to the central star is $v = \sqrt{GM_\star/r}$, where G is Newton's gravitational constant. In the z direction vertical to the disk, the gas pressure is balanced with the gravitational force, i.e.,

$$\frac{1}{\rho}\frac{\partial P}{\partial z} = -\frac{GM_\star z}{r^3}, \tag{15}$$

where ρ and P are the density and pressure of the matter, respectively. The height $H(r)$ at radius r is estimated by

$$H(r) \simeq c_{\rm s}\left(\frac{r}{GM_\star}\right)^{1/2} r, \tag{16}$$

with the isothermal sound speed $c_s = (kT/\mu_{\rm m}m_{\rm H})^{1/2}$, where $\mu_{\rm m} = 0.61$ is the mean molecular weight for a solar composition, T is the isothermal electron temperature, and $m_{\rm H}$ is the mass of hydrogen. The temperature of the disk is roughly constant, $T \sim 2 \times 10^4$ K, within 100 $R_\star$ in the radial direction (e.g., Millar & Marlborough 1998, 1999). The density structure of the Be star disk can be represented radially as a power law and vertically with an exponential decay (e.g., McGill et al. 2013), i.e.,

$$\rho(r, z) = \rho_0\left(\frac{r}{R_\star}\right)^{-\eta} e^{-(z/H(r))^2}, \tag{17}$$

where the base density ρ_0 for most of the Be stars ranges from 10^{-13} to 10^{-10} g cm^{-3} (e.g., Carciofi et al. 2007; Jones et al. 2008; Tycner et al. 2008), and the index η ranges from 2 to 5 (e.g., Waters et al. 1987; Dougherty et al. 1994)

In order to calculate the optical depth of a burst along a certain propagation direction, we first define the direction vector of the line of sight. In the reference frame centered on the Be star, the direction vector of the line of sight can be expressed as $(\cos(\beta_0)\cos(\alpha_0), \cos(\beta_0)\sin(\alpha_0), \sin(\beta_0))$, with a direction angle α_0 and vertical angle β_0. When the NS moves in the disk of the Be star, the optical depth of free–free absorption along the line of sight is calculated by

$$\tau_\nu = \int \kappa_\nu dl, \tag{18}$$

with the attenuation coefficient (e.g., Draine 2011)

$$\begin{aligned}\kappa_\nu &\approx 1.772 \times 10^{-26} T_4^{-1.5} \nu_9^{-2} Z_i^2 g_{\rm ff} n_e n_i \text{ cm}^{-1} \\ &\approx 1.091 \times 10^{-25} Z_i^{1.882} T_4^{-1.323} \nu_9^{-2.118} n_e n_i \text{ cm}^{-1},\end{aligned} \tag{19}$$

where $T = T_4 10^4$ K is the temperature, $\nu = \nu_9 10^9$ Hz is the frequency, $Z_i \sim 1$ is the charge of ions, $g_{\rm ff}(\nu, T)$ is the Gaunt factor for the free–free emission, and $n_i \approx n_e$ is assumed with the ion density n_i and electron density $n_e = \rho/\mu_e m_{\rm H}$, with the mean molecular weight per electron $\mu_e = 1.2$ for a solar composition. If $\tau_\nu > 1$, the observed flux of an FRB would be significantly reduced by free–free absorption. According to Equation (18), in the following part, we will calculate the burst rate at different frequencies from a certain propagation path after the free–free absorption.

When the NS is in the Be star disk, it will accrete the material and trigger FRBs by starquakes, as discussed in Section 2.1. We assume the burst rate during the active window satisfying a Gaussian distribution as a function of phase (also see the observation result of Figure 4 in Pastor-Marazuela et al. 2020). The burst rate reaches the maximum near the periastron and decreases when the NS is away from the periastron because the accretion rate depends on the density of the Be star disk. Such a Gaussian burst rate is also consistent with pulse shapes of type I outbursts of BeXRBs (e.g., Wilson et al. 2002; Baykal et al. 2008; Wilson et al. 2008). The burst rate at 1 GHz as a function of phase can be represented by

$$\mathcal{R}_{1\text{ GHz}}(\phi) = \mathcal{R}_0 \frac{1}{\sigma_\phi\sqrt{2\pi}} e^{-\frac{(\phi-\phi_0)^2}{2\sigma_\phi^2}}, \tag{20}$$

where $\mathcal{R}_0$ is the normalized constant, σ_ϕ is the standard deviation, and $\phi_0 = 0.5$. According to Extended Figure 1 of Pastor-Marazuela et al. (2020), for bursts of the same fluence, FRB 180916B is around over an order of magnitude more active at 150 MHz than at 1.4 GHz. Thus, the ratio of burst rates in 1.4 GHz and 150 MHz is $\mathcal{R}_{1.4\text{ GHz}}/\mathcal{R}_{150\text{ MHz}} = (1.4\text{ GHz}/150\text{ MHz})^{-1}$. Furthermore, we assume that the burst rate at different frequencies can be represented by

$$\mathcal{R}_\nu(\phi) = \mathcal{R}_{1\text{ GHz}}(\phi)\left(\frac{\nu}{1\text{ GHz}}\right)^\alpha, \tag{21}$$

with $\alpha \approx -1$ as a typical value.

We further generate a sample of FRBs with different frequencies at different phases. The fluences of FRBs, $f_\nu(\phi)$, at a phase ϕ are assumed to satisfy a normal distribution of $N(\mu_{f_\nu}, \sigma^2_{f_\nu})$, where μ_{f_ν} is the average fluence and σ_{f_ν} is the standard deviation. According to Extended Figure 1 of Pastor-Marazuela et al. (2020), the fluence of the low-frequency bursts is higher than that of the high-frequency bursts. The average fluence at 1.4 GHz of FRB 180916B is a few jansky milliseconds; however, at 150 MHz, it is a few hundred jansky milliseconds. We assume the average fluence at different frequencies ν as a power law, i.e.,

$$\mu_{f_\nu} = \mu_{f_{1\,\mathrm{GHz}}} \left(\frac{\nu}{1\ \mathrm{GHz}} \right)^{\gamma}, \tag{22}$$

where $\mu_{f_{1\,\mathrm{GHz}}}$ is the average fluence at 1 GHz, and γ is the power-law index, with $\gamma \approx -2$ as a typical value.

Involving the absorption of the disk of the Be star, the observed fluence of each burst at phase ϕ can be estimated by

$$f_{\nu,\mathrm{obs}}(\phi) = f_\nu(\phi) e^{-\tau_\nu(\phi)}. \tag{23}$$

The observed burst rate $\mathcal{R}_{\nu,\mathrm{obs}}$ is determined by the fluence threshold of a specific telescope. When the $f_{\nu,\mathrm{obs}}(\phi)$ of a burst is greater than the threshold, it is regarded as observable. The thresholds of Apertif, CHIME, and LOFAR are about 1 (Pastor-Marazuela et al. 2020), 5.3 (CHIME/FRB Collaboration et al. 2020a), and 50 Jy ms (Pastor-Marazuela et al. 2020), respectively. Next, in order to explain the activity window of FRB 180916B, we will simulate the observable active window of FRBs affected by the free–free absorption of the disk of the Be star.

In general, the radius of Be stars, $R_\star$, ranges from $\sim$3 to $\sim$13 $R_\odot$, and the radius of the Be star disk, R_{disk}, ranges from about 1.5 to 17 $R_\star$ (Rivinius et al. 2013). The mass of the Be star is $>8\,M_\odot$ (Reig 2011). The eccentricity of binary orbits can be 0.1–0.9 (Ziolkowski 2002). If the central star is a B0 main-sequence star, the typical parameters are $R_\star = 7.41\ R_\odot$ and $M_\star = 17.8\,M_\odot$ (Allen 1973). In order to explain the observation properties of the frequency-dependent active window of FRB 180916B, we find that the following parameters are appropriate: the radius of the Be star is $R_\star = 5\ R_\odot$, the mass of the Be star is $M_\star = 15\ M_\odot$, the temperature of the disk is $T = 2 \times 10^4$ K, the index of the density structure of the disk is $\eta = 4.5$, the base density of the density structure is $\rho_0 = 1.6 \times 10^{-13}$ g cm^{-3}, the orbital eccentricity is $e = 0.35$, the standard deviation of the burst rate is $\sigma_\phi = 0.065$, the reference burst rate is $\mathcal{R}_0 = 100$ h^{-1}, the index of the burst rate with frequency is $\alpha = -1.0$, the average fluence of bursts at 1 GHz is $\mu_{f_{1\,\mathrm{GHz}}} = 5$ Jy ms, the standard deviation of the fluence of bursts is $\sigma_{f_\nu} = 0.3\mu_{f_\nu}$, the power-law index of the average fluence with frequency is $\gamma = -2.0$, and the direction of the burst is $\alpha_0 = -0.7\pi$ and $\beta_0 = -0.05\pi$. Then the disk of the Be star is about 67.4 $R_\odot$. The frequency-dependent burst rate with phase is shown in Figure 4. We can see that the peaks of the active windows of high- and low-frequency bursts appear at different phases. Low-frequency bursts are observed later than high-frequency bursts in an orbital cycle. Bursts with a frequency of 600 MHz have a wider periodic activity window. The dotted red line denotes the burst rate at 150 MHz. Because of the absorption, it has the greatest influence on the 150 MHz bursts, and the burst rate at 600 MHz does not follow the shape of the Gaussian model. The above results are consistent with the observation properties of FRB 180916B.

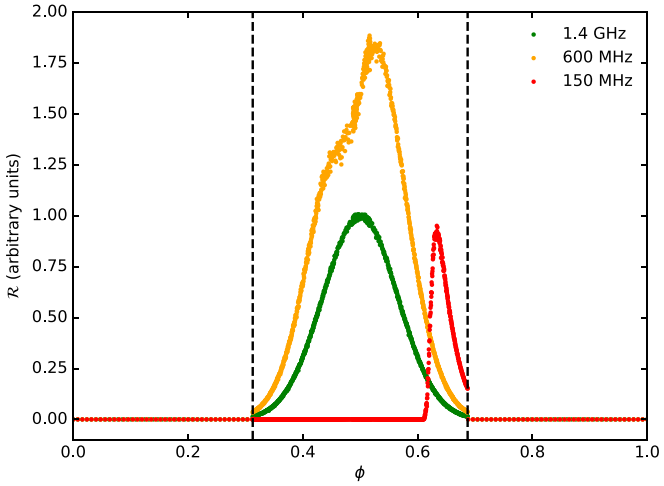

Figure 4. Simulation result of the burst rate with phase due to free–free absorption of the Be star disk. The burst rate is plotted in arbitrary units. The dotted green, orange, and red lines denote bursts rate at 1.4 GHz, 600 MHz, and 150 MHz, respectively. The range between the two dashed black lines indicates that the NS is in the Be star disk, and it is the active window of bursts in the BeXRB system. The parameters are taken as $R_\star = 5\ R_\odot$, $M_\star = 15\ M_\odot$, $T = 2 \times 10^4$ K, $\eta = 4.5$, $\rho_0 = 1.6 \times 10^{-13}$ g cm^{-3}, $e = 0.35$, $\alpha = -1.0$, $\sigma_\phi = 0.065$, $\mathcal{R}_0 = 100$ h^{-1}, $\mu_{f_{1\,\mathrm{GHz}}} = 5$ Jy ms, $\sigma_{f_\nu} = 0.3\mu_{f_\nu}$, $\gamma = -2.0$, $\alpha_0 = -0.7\pi$, and $\beta_0 = -0.05\pi$.

2.3. The DM Contribution from the Be Star Disk

When the NS is in the Be star disk, the observed DM will also change with orbit phase. In general, the total observed DM can be divided into (Deng & Zhang 2014; Zhang 2018) $\mathrm{DM_{tot}} = \mathrm{DM_{MW}} + \mathrm{DM_{IGM}} + (\mathrm{DM_{host}} + \mathrm{DM_{src}})/(1+z)$, where $\mathrm{DM_{MW}}$ and $\mathrm{DM_{IGM}}$ are the contributions from the Milky Way and intergalactic medium, respectively; $\mathrm{DM_{host}}$ and $\mathrm{DM_{src}}$ are the contributions from the host galaxy and source local environment in the rest frame of the FRB, respectively; and z is the redshift of the FRB. Yang & Zhang (2017) investigated the various possibilities that may cause DM variations of an FRB and found that only the near-source plasma can cause observable DM variations. In a BeXRB system, we mainly consider the DM variations contributed from $\mathrm{DM_{src}}$, i.e., $\mathrm{DM_{disk}}$, the DM contribution from the Be star disk.

Different from an observable increasing DM of FRB 121102 (e.g., Oostrum et al. 2020; Zhao et al. 2021), there is no obvious DM variation with phase for FRB 180916B, and the largest DM variation is about 4 pc cm^{-3} (see top panel of Extended Figure 7 in Pastor-Marazuela et al. 2020). Based on the density profile of the Be star disk, Equation (17), we obtain $\mathrm{DM_{disk}}$ at different phases, as shown in Figure 5. The parameters are taken to be the same as in Figure 4. The red part corresponds to the DM in the active window, and the blue part corresponds to the DM in the nonactive window. In the nonactive window, since the NS moves out of the Be star disk, the burst rate is much lower, according to Equation (12), although it may appear a slight DM variation. For the given parameters satisfying the properties of the observed frequency-dependent active window of FRB 180916B, we find that the DM contribution from the Be star disk is <1 pc cm^{-3}.

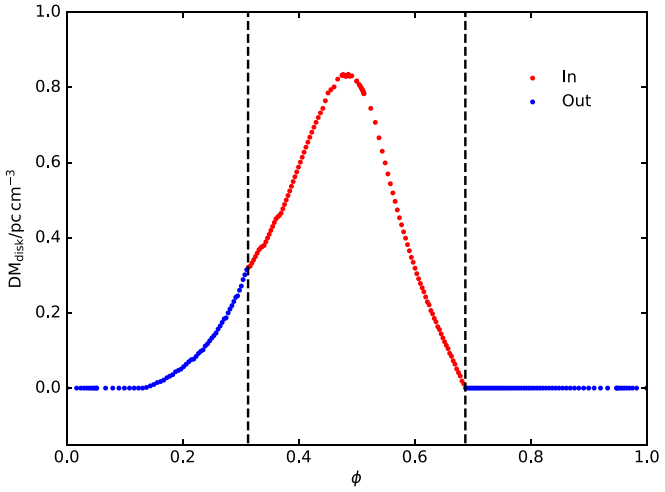

Figure 5. DM contribution of the Be star disk at different phases. The range between the two dashed black lines denotes that the NS is in the Be star disk. The dotted red and blue lines denote DM_{disk} when the NS is in/outside the Be star disk, respectively. The parameters are the same as in Figure 4, i.e., $R_\star = 5\ R_\odot$, $M_\star = 15\ M_\odot$, $T = 2 \times 10^4$ K, $\eta = 4.5$, $\rho_0 = 1.6 \times 10^{-13}$ g cm^{-3}, $e = 0.35$, $\alpha_0 = -0.7\pi$, and $\beta_0 = -0.05\pi$.

3. Discussion and Conclusions

Recently, FRB 180916B was found to appear frequency-dependent activities with a period of 16.35 days (CHIME/FRB Collaboration et al. 2019). Such a period might correspond to the orbit period of a binary system (Dai et al. 2016; Smallwood et al. 2019; Ioka & Zhang 2020; Lyutikov et al. 2020; Mottez et al. 2020; Dai & Zhong 2020; Gu et al. 2020; Decoene et al. 2021; Deng et al. 2021; Kuerban et al. 2021; Wada et al. 2021). The FRB 180916B is ∼250 pc offset from the brightest region of the nearest young stellar clump in its host galaxy. The large offset is in tension with scenarios that invoke young magnetars born from core-collapse supernovae but well consistent with the case of the HMXBs.

In this work, we propose that a BeXRB system might be the source of a repeating FRB with periodic activities. When the NS accretes the material of the Be star disk, the interaction between the NS magnetosphere and the accreted material results in the spin evolution of the NS, leading to the stress in the NS crust increased. When the stress of the crust reaches the critical value, a starquake occurs and further produces FRBs. The Alfvén waves are launched by starquakes and convert to coherent radio emission at a distance of a few tens of NS radii (Kumar & Bošnjak 2020; Lu et al. 2020; Yang & Zhang 2021). The interval between starquakes is estimated to be a few days. When the NS is not in the disk of the Be star, due to the long waiting time, the radio bursts occurring at the nonactive phase will be too rare to be observed. With the observed burst rate of FRB 180916B, we can constrain the period and magnetic field of the NS to the limited parameter space.

On the other hand, we study the frequency-dependent active window of FRB 180916B in the above scenario. When the NS is in the disk of the Be star, the optical depth of free–free absorption along the line of sight will evolve with orbit phase. If the optical depth is larger than unity, the observed flux of an FRB would be significantly reduced. The FRBs with fluences lower than the telescope threshold would not be observable. Since the free–free absorption is frequency-dependent, the observed active window of FRBs would be frequency-dependent naturally. Based on the simulation of our model, we find that the active windows of high- and low-frequency bursts peak at different phases, as shown in Figure 4. Low-frequency bursts are observed later than high-frequency bursts in an orbital cycle, which is consistent with the observation properties of FRB 180916B. We also evaluate the DM contribution from the Be star disk. It is lower than 1 pc cm^{-3} when the NS is in the Be star disk, which is also consistent with the observation of FRB 180916B.

It is noteworthy that several more parameters could affect the features of FRBs with periodic activities. For instance, the waiting time between bursts is inversely proportional to the strength of the magnetic field, the accretion rate, and the spin angular velocity of the NS. Meanwhile, the active window will be shorter if the orbital eccentricity is larger for a given semimajor axis. The profile of the burst rate in the active window will also depend on the length of the semimajor axis of the orbit.

In this model involving the BeXRB, repeating FRBs with periodic activities might be produced by the NS crust fracturing adjusted by the balance between crust stress and NS spin. To satisfy the observed high burst rate of FRB 180916B, i.e., the waiting time of starquakes induced by accretion <6.1 days and radiation >16.29 days, the NS should have a fast spin period of $P_{\rm NS} \sim 0.02$ s, a relative large surface magnetic field of $B_{\rm NS} \sim 10^{13}$ G, and a small oblateness variation of $\Delta\epsilon \sim 10^{-13}$. Such an NS in the BeXRB system is allowable but relatively rare, which might explain why most Galactic BeXRBs do not show FRBs. On the other hand, in the BeXRB scenario, the multiwavelength counterparts of FRBs could be type I outbursts. However, since most FRBs occur at cosmological distances, the FRB-associated type I outbursts would be hard to detect. The FRB-associated type I outbursts with a typical luminosity of 10^{36}–10^{37} erg s^{-1} could be detected within a distance of $\lesssim$30 kpc for current main X-ray detectors, such as Insight-HXMT (Zhang et al. 2018).

We thank the anonymous referee for providing helpful comments and suggestions. We also thank Qian-Cheng Liu, Bin Hong, and Qin Han for helpful discussions. This work was supported by the National Key Research and Development Program of China (grant No. 2017YFA0402600), the National SKA Program of China (grant No. 2020SKA0120300), and the National Natural Science Foundation of China (grants 11833003, U1831207, and 11988101). Y.P.Y. is supported by National Natural Science Foundation of China grant No. 12003028.

ORCID iDs

Qiao-Chu Li https://orcid.org/0000-0003-0855-3649
Yuan-Pei Yang https://orcid.org/0000-0001-6374-8313
F. Y. Wang https://orcid.org/0000-0003-4157-7714
Kun Xu https://orcid.org/0000-0002-9739-8929
Yong Shao https://orcid.org/0000-0003-2506-6906
Zi-Gao Dai https://orcid.org/0000-0002-7835-8585

References

Aggarwal, K., Law, C. J., Burke-Spolaor, S., et al. 2020, RNAAS, 4, 94
Allen, C. W. 1973, Astrophysical Quantities (3rd ed.; London: Univ. London, Athlone Press)
Bannister, K. W., Deller, A. T., Phillips, C., et al. 2019, Sci, 365, 565
Baykal, A., Kızıloğlu, Ü, Kızıloğlu, N., et al. 2008, A&A, 479, 301
Baym, G., & Pines, D. 1971, AnPhy, 66, 816
Beloborodov, A. M. 2020, ApJ, 896, 142
Beniamini, P., Wadiasingh, Z., & Metzger, B. D. 2020, MNRAS, 496, 3390

Bochenek, C. D., Ravi, V., Belov, K. V., et al. 2020, Natur, 587, 59
Bodaghee, A., Tomsick, J. A., Rodriguez, J., et al. 2012, ApJ, 744, 108
Carciofi, A. C., Magalhães, A. M., Leister, N. V., et al. 2007, ApJL, 671, L49
Chatterjee, S., Law, C. J., Wharton, R. S., et al. 2017, Natur, 541, 58
CHIME/FRB Collaboration, Amiri, M., Andersen, B. C., et al. 2020a, Natur, 582, 351
CHIME/FRB Collaboration, Amiri, M., Bandura, K., et al. 2019, Natur, 566, 235
CHIME/FRB Collaboration, Andersen, B. C., Bandura, K. M., et al. 2020b, Natur, 587, 54
Cordes, J. M., & Chatterjee, S. 2019, ARA&A, 57, 417
Cruces, M., Spitler, L. G., Scholz, P., et al. 2021, MNRAS, 500, 448
Cusumano, G., Maccarone, M. C., Nicastro, L., et al. 2000, ApJL, 528, L25
Dai, Z. G. 2020, ApJL, 897, L40
Dai, Z. G., Wang, J. S., Wu, X. F., et al. 2016, ApJ, 829, 27
Dai, Z. G., & Zhong, S. Q. 2020, ApJL, 895, L1
Decoene, V., Kotera, K., & Silk, J. 2021, A&A, 645, A122
Deng, C.-M., Zhong, S.-Q., & Dai, Z.-G. 2021, arXiv:2102.06796
Deng, W., & Zhang, B. 2014, ApJL, 783, L35
Douchin, F., & Haensel, P. 2001, A&A, 380, 151
Dougherty, S. M., Waters, L. B. F. M., Burki, G., et al. 1994, A&A, 290, 609
Draine, B. T. 2011, Physics of the Interstellar and Inter Medium (Princeton, NJ: Princeton Univ. Press)
Espinoza, C. M., Lyne, A. G., Stappers, B. W., et al. 2011, MNRAS, 414, 1679
Filippova, E. V., Mereminskiy, I. A., Lutovinov, A. A., et al. 2017, AstL, 43, 706
Frank, J., King, A., & Raine, D. J. 2002, Accretion Power in Astrophysics, by Juhan Frank and Andrew King and Derek Raine (Cambridge: Cambridge Univ. Press), 398
Geng, J. J., & Huang, Y. F. 2015, ApJ, 809, 24
Geng, J.-J., Li, B., Li, L.-B., et al. 2020, ApJL, 898, L55
Geng, J., Li, B., & Huang, Y. 2021, The Innovation, 2, 100152
Ghosh, P., & Lamb, F. K. 1979a, ApJ, 232, 259
Ghosh, P., & Lamb, F. K. 1979b, ApJ, 234, 296
Gu, W.-M., Yi, T., & Liu, T. 2020, MNRAS, 497, 1543
Haensel, P., & Zdunik, J. L. 2008, A&A, 480, 459
Haskell, B., & Melatos, A. 2015, IJMPD, 24, 1530008
Ikhsanov, N. R. 2007, MNRAS, 375, 698
Ioka, K., & Zhang, B. 2020, ApJL, 893, L26
Jones, C. E., Tycner, C., Sigut, T. A. A., et al. 2008, ApJ, 687, 598
Kaaret, P., Piraino, S., Halpern, J., et al. 1999, ApJ, 523, 197
Katz, J. I. 2018, MNRAS, 481, 2946
Kuerban, A., Huang, Y.-F., Geng, J.-J., et al. 2021, arXiv:2102.04264
Kumar, P., & Bošnjak, Ž. 2020, MNRAS, 494, 2385
Kumar, P., Lu, W., & Bhattacharya, M. 2017, MNRAS, 468, 2726
Kumar, P., Shannon, R. M., Osłowski, S., et al. 2019, ApJL, 887, L30
Lai, X. Y., Yun, C. A., Lu, J. G., et al. 2018, MNRAS, 476, 3303
Lee, U., Osaki, Y., & Saio, H. 1991, MNRAS, 250, 432
Levin, Y., Beloborodov, A. M., & Bransgrove, A. 2020, ApJL, 895, L30
Li, C. K., Lin, L., Xiong, S. L., et al. 2021, NatAs, 5, 378
Li, D., & Zanazzi, J. J. 2021, ApJL, 909, L25
Lorimer, D. R., Bailes, M., McLaughlin, M. A., et al. 2007, Sci, 318, 777
Lü, G.-L., Zhu, C.-H., Postnov, K. A., et al. 2012, MNRAS, 424, 2265
Lu, W., Kumar, P., & Zhang, B. 2020, MNRAS, 498, 1397
Luo, R., Wang, B. J., Men, Y. P., et al. 2020, Natur, 586, 693
Lyubarsky, Y. 2014, MNRAS, 442, L9
Lyutikov, M. 2017, ApJL, 838, L13
Lyutikov, M., Barkov, M. V., & Giannios, D. 2020, ApJL, 893, L39
Marcote, B., Nimmo, K., Hessels, J. W. T., et al. 2020, Natur, 577, 190
Marthi, V. R., Gautam, T., Li, D. Z., et al. 2020, MNRAS, 499, L16
McGill, M. A., Sigut, T. A. A., & Jones, C. E. 2013, ApJS, 204, 2
Mereghetti, S., Savchenko, V., Ferrigno, C., et al. 2020, ApJL, 898, L29
Metzger, B. D., Margalit, B., & Sironi, L. 2019, MNRAS, 485, 4091
Millar, C. E., & Marlborough, J. M. 1998, ApJ, 494, 715
Millar, C. E., & Marlborough, J. M. 1999, ApJ, 516, 276
Mottez, F., Zarka, P., & Voisin, G. 2020, A&A, 644, A145
Okazaki, A. T. 1991, PASJ, 43, 75
Okazaki, A. T., Bate, M. R., Ogilvie, G. I., et al. 2002, MNRAS, 337, 967
Okazaki, A. T., & Negueruela, I. 2001, A&A, 377, 161
Oostrum, L. C., Maan, Y., van Leeuwen, J., et al. 2020, A&A, 635, A61
Pastor-Marazuela, I., Connor, L., van Leeuwen, J., et al. 2020, arXiv:2012.08348
Petroff, E., Hessels, J. W. T., & Lorimer, D. R. 2019, A&ARv, 27, 4
Piro, A. L. 2005, ApJL, 634, L153
Platts, E., Weltman, A., Walters, A., et al. 2019, PhR, 821, 1
Pleunis, Z., Michilli, D., Bassa, C. G., et al. 2021, ApJL, 911, L3
Prochaska, J. X., Macquart, J.-P., McQuinn, M., et al. 2019, Sci, 366, 231
Quirrenbach, A., Bjorkman, K. S., Bjorkman, J. E., et al. 1997, ApJ, 479, 477
Rajwade, K. M., Mickaliger, M. B., Stappers, B. W., et al. 2020, MNRAS, 495, 3551
Ravi, V., Catha, M., D'Addario, L., et al. 2019, Natur, 572, 352
Reig, P. 2011, Ap&SS, 332, 1
Ridnaia, A., Svinkin, D., Frederiks, D., et al. 2021, NatAs, 5, 372
Rivinius, T., Carciofi, A. C., & Martayan, C. 2013, A&ARv, 21, 69
Sand, K. R., Gajjar, V., Pilia, M., et al. 2020, ATel, 13781, 1
Shakura, N., Postnov, K., Kochetkova, A., et al. 2012, MNRAS, 420, 216
Shapiro, S. L., & Teukolsky, S. A. 1983, Black holes, White Dwarfs, and Neutron Stars: The Physics of Compact Objects (New York: Wiley)
Smallwood, J. L., Martin, R. G., & Zhang, B. 2019, MNRAS, 485, 1367
Spitler, L. G., Cordes, J. M., Hessels, J. W. T., et al. 2014, ApJ, 790, 101
Spitler, L. G., Scholz, P., Hessels, J. W. T., et al. 2016, Natur, 531, 202
Sridhar, N., Metzger, B. D., Beniamini, P., et al. 2021, ApJ, 917, 13
Tauris, T. M., & van den Heuvel, E. P. J. 2006, in Compact Stellar X-ray Sources, ed. W. Lewin & M. van der Klis (Cambridge: Cambridge Univ. Press), 626
Tavani, M., Casentini, C., Ursi, A., et al. 2021, NatAs, 5, 401
Taylor, J. H., Manchester, R. N., & Lyne, A. G. 1993, ApJS, 88, 529
Tendulkar, S. P., Gil de Paz, A., Kirichenko, A. Y., et al. 2021, ApJL, 908, L12
Thompson, C., & Duncan, R. C. 1995, MNRAS, 275, 255
Thornton, D., Stappers, B., Bailes, M., et al. 2013, Sci, 341, 53
Tong, H., Wang, W., & Wang, H.-G. 2020, RAA, 20, 142
Tycner, C., Jones, C. E., Sigut, T. A. A., et al. 2008, ApJ, 689, 461
Wada, T., Ioka, K., & Zhang, B. 2021, arXiv:2105.14480
Wadiasingh, Z., & Timokhin, A. 2019, ApJ, 879, 4
Waters, L. B. F. M., Cote, J., & Lamers, H. J. G. L. M. 1987, A&A, 185, 206
Waxman, E. 2017, ApJ, 842, 34
Wilson, C. A., Finger, M. H., & Camero-Arranz, A. 2008, ApJ, 678, 1263
Wilson, C. A., Finger, M. H., Coe, M. J., et al. 2002, ApJ, 570, 287
Wilson-Hodge, C. A., Malacaria, C., Jenke, P. A., et al. 2018, ApJ, 863, 9
Wu, Q., Zhang, G. Q., Wang, F. Y., et al. 2020, ApJL, 900, L26
Xiao, D., & Dai, Z.-G. 2020, ApJL, 904, L5
Xiao, D., Wang, F. Y., & Dai, Z.-G. 2021, SCPMA, 64, 249501
Xu, K., Li, Q.-C., Yang, Y.-P., et al. 2021, ApJ, 917, 2
Xu, X.-T., & Li, X.-D. 2019, ApJ, 872, 102
Yang, H., & Zou, Y.-C. 2020, ApJL, 893, L31
Yang, Y.-P., & Zhang, B. 2017, ApJ, 847, 22
Yang, Y.-P., & Zhang, B. 2018, ApJ, 868, 31
Yang, Y.-P., & Zhang, B. 2021, arXiv:2104.01925
Yang, Y.-P., Zhu, J.-P., Zhang, B., et al. 2020, ApJL, 901, L13
Yu, Y.-W., Zou, Y.-C., Dai, Z.-G., et al. 2021, MNRAS, 500, 2704
Zanazzi, J. J., & Lai, D. 2020, ApJL, 892, L15
Zdunik, J. L., Bejger, M., & Haensel, P. 2008, A&A, 491, 489
Zhang, B. 2017, ApJL, 836, L32
Zhang, B. 2018, ApJL, 867, L21
Zhang, B. 2020a, Natur, 582, 344
Zhang, B. 2020b, Natur, 587, 45
Zhang, G. Q., Tu, Z.-L., & Wang, F. Y. 2021, ApJ, 909, 83
Zhang, S., Zhang, S. N., Lu, F. J., et al. 2018, Proc. SPIE, 10699, 106991U
Zhang, X., & Gao, H. 2020, MNRAS, 498, L1
Zhao, Z. Y., Zhang, G. Q., Wang, Y. Y., et al. 2021, ApJ, 907, 111
Ziolkowski, J. 2002, MmSAI, 73, 1038
Zou, J.-H., Zhang, B.-B., Zhang, G.-Q., et al. 2021, arXiv:2107.03800